$\boxed{\textbf{Final Homework Assignment}}$

<u>Due date</u>: Friday, 4 March 2022 at 5 PM

M. Jabbour

1 Isothermal solidification of a liquid mixture

<u>Background:</u> During the solidification of a binary alloy from its melt, the diffusion of one of the two chemical species (referred to hereafter as the solute) controls the evolution of the front in the same way heat conduction governs the motion of the interface between liquid and solid phases in a pure substance. Specifically, since heat conduction is much faster than chemical diffusion, temperature variations occur on a time scale much shorter than that which characterizes the rearrangement by diffusion of species. Consequently, solidification in alloys can be approximated as *isothermal*. Further, if the solubility of the diffusing species is smaller in the solid than it is in the liquid, the advancing solidification front in a binary alloy rejects solute molecules, in much the same manner it releases latent heat in the thermal case of a solidifying pure substance. The rate at which this excess solute is transported by diffusion away from the interface determines how rapidly the solidification proceeds.
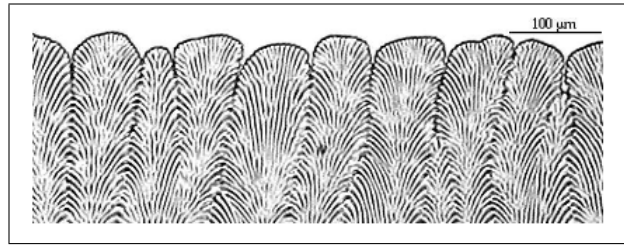

Figure 1: So-called eutectic colonies are two-phase lamellar cells that are commonly observed during the solidification of ternary alloys (here, the binary alloy CBr_4–C_2Cl_6 doped with a small fraction of naphtalene impurity). These periodically distributed lamellar plates consist of rods of one solid phase of the binary alloy embedded in a matrix of the other solid phase. The formation of this microstructure is triggered by a morphological instability of a macroscopically planar solidification front, due to the rejection by both solid phases of the ternary impurity and its diffusion into the liquid. [Reproduced from S. Akamatsu and G. Faivre, *Physical Review E* **61**, 3757 (2000); see also M. Plapp and A. Karma, *Physical Review E* **66**, 061608 (2002).]

<u>Setting:</u> In this problem, we model the solidification of a binary alloy from its melt by specializing the theory derived in class for diffusion-driven phase transformations to situations in which all mechanical work is negligible. Hence, the coupling between solute diffusion and stress is ignored, which is tantamount to assuming that the liquid and solid phases cannot deform. Specifically, let μ_0 be the *transition potential*, i.e., μ_0 is the unique solution of

$$\omega_\ell(\mu_0) = \omega_s(\mu_0), \tag{1}$$

and define the dimensionless chemical-potential difference u in each of the solid and liquid phases

as

$$u_i := \frac{\mu_i - \mu_0}{\mu_0} \quad (i = s, \ell). \tag{2}$$

In what follows, we consider, as we did in class, bulk grand canonical potentials that are *affine* functions of μ, i.e.,

$$\omega_i(\mu) = \omega_i(\mu_0) + \mu_0 \Gamma_i u \quad (i = s, \ell). \tag{3}$$

1.1. Let $\Omega_i(t)$ be the region occupied at time t by the i phase $(i = s, \ell)$ and denote by $\mathcal{S}(t)$ the evolving solidification front. Show that the free-boundary problem for the evolution of the solidification front reduces to Laplace's equation in each of the two phases

$$\nabla^2 u_i = 0 \quad \text{in } \Omega_i(t) \quad (i = s, \ell), \tag{4}$$

supplemented by the interfacial mass balance

$$v_n^* = -(\overline{M}_\ell (\nabla u_\ell)^+ - \overline{M}_s (\nabla u_s)^-) \cdot \boldsymbol{n}^* \quad \text{along } \mathcal{S}(t), \tag{5}$$

where the rescaled solute mobility $\overline{M}_i$ in the i phase is given by

$$\overline{M}_i := \frac{M_i}{\mu_0 (\Gamma_s - \Gamma_\ell)} \quad (i = s, \ell), \tag{6}$$

and the (generalized) Gibbs–Thomson relation

$$u = \psi \kappa^* - \frac{v_n^*}{\beta} \quad \text{along } \mathcal{S}(t), \tag{7}$$

with the rescaled interfacial free-energy density ψ and kinetic mobility β defined as

$$\psi := \frac{\psi^*}{\mu_0 (\Gamma_s - \Gamma_\ell)} \quad \text{and} \quad \beta := \mu_0 (\Gamma_s - \Gamma_\ell) \beta^*. \tag{8}$$

Hence, as with temperature during the solidification of a pure substance, the solute chemical potential μ, which in (7) is assumed to be *continuous* across the moving interface, is different from its transition value μ_0 defined in (1). One contribution to this difference, $\psi \kappa^*$, is energetic and due to capillarity, while the other contribution, $-\frac{v_n^*}{\beta}$, is dissipative and associated with the kinetics of the phase transformation.

1.2. As a result of its higher solubility in the liquid, the density of solute molecules in the liquid phase is higher than their density in the solid phase. Show that $\Gamma_\ell < \Gamma_s$, so that $\overline{M}_i > 0$ for $i = s, \ell$.

Further, show that if the solid phase occupies a *convex* region, the solute chemical potential at the interface has to be *below* its transition value for the solidification front to advance into the liquid phase.

1.3. In what follows, we solve the free-boundary problem (4), (5), and (7), supplemented by appropriate initial and boundary conditions, in order to gain insight into the isothermal growth of a solid seed in a binary liquid. To do so, consider a disk $\mathfrak{D}$, centered at the origin and of radius R_e, filled with the melt of the binary alloy under consideration. Suppose that the diffusive flux of solute molecules is prescribed at the boundary of the disk:

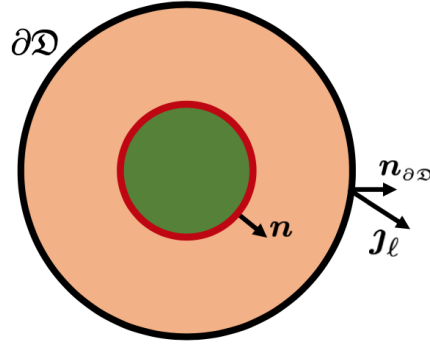$$\boldsymbol{\jmath}_\ell \cdot \boldsymbol{n}_{\partial \mathfrak{D}} = \jmath_e, \tag{9}$$

Figure 2: At time t, the solid occupies the disk of radius $R(t)$ (shown in green) and the liquid the annulus of outer radius R_e (shown in orange). The unit normal $\boldsymbol{n}$ to the interface (shown in red) points into the liquid.

with $\boldsymbol{n}_{\partial\mathfrak{D}}$ the outward normal to the boundary and $\jmath_e$ is a given constant. (Note that when the solute flows out of the disk, $\jmath_e > 0$.)

We are concerned with the growth of a solid seed that initially occupies a single point at the center of the disk. We seek *radially symmetric* solutions, so that the solid-liquid interface is given by $r = R(t)$, where $t \in [0, t_*]$ and t_* remains to be specified. Hence, at time t, the solid is identified with the disk centered at the origin and of radius $R(t)$, and the liquid occupies the annulus centered at the origin, of inner radius $R(t)$ and outer radius R_e (see Fig. 2). Laplace's equation (4) in the bulk phases, the interfacial solute balance (5), and the generalized Gibbs–Thomson relation (7) are supplemented by the boundary condition (9) and the initial condition

$$R(0) = 0. \tag{10}$$

By choosing a parametrization of the interface such that its unit normal $\boldsymbol{n}^*$ points into the liquid, show that

$$v_n^* = \dot{R}(t) \quad \text{and} \quad \kappa^* = -\frac{1}{R(t)} < 0, \tag{11}$$

where the superimposed dot denotes time differentiation.

1.4. Solve the boundary-value problem consisting of Laplace's equation (4) in each of the solid and liquid phases, the condition (9) at the outer boundary, and the Gibbs–Thomson relation (7) at the interface.

1.5. Determine the position $R(t)$ of the solidification front at time t. In particular, show that the solid seed can grow only if $\jmath_e > 0$, i.e., solute molecules are removed from the liquid at the boundary. In this case, show that the the solute chemical potential in the liquid satisfies

$$\mu_\ell(r, t) < \mu_0 \quad \forall\, r \in (R(t), R_e). \tag{12}$$

Compute the time t_* at which the entire disk has solidified. Finally, can we expect a steady-state chemical potential if we continue to remove solute molecules at the boundary?

2   Diffusion-driven transformation in a two-phase elastic bar

Background: In class, we developed a continuum sharp-interface theory for diffusion-driven transformations in two-phase elastic solids, with the transition kinetics governed by the interplay between transport of a chemical species and stress. There are many technologically relevant examples of such phase transformations, including the two-phase lithiation of anodes in Li-ion batteries, as shown in Fig. 3.
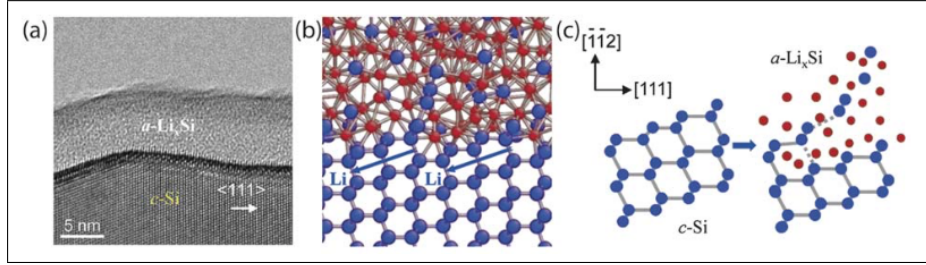

Figure 3: **(a)** High-resolution transmission electron microscopy of the sharp interface between a crystalline silicon phase and an amorphous lithiated-silicon phase $Li_x Si$ ($x = 3.5$). **(b)** Snapshot from a molecular-dynamics simulation showing the atomic structures of the two phases near the interface, with the silicon atoms in blue and the lithium atoms in red. **(c)** High lithium concentrations at the phase boundary facilitate the breaking of Si–Si bonds. [Reproduced from J. W. Wang et al. *Nano Letters* **13**, 709–715 (2013).]

Setting: We consider the specialization of the aforementioned theory to the one-dimensional setting of a two-phase linearly elastic bar which, after rescaling, occupies the segment $[0, 1]$ of the x-axis, see Fig. 4 below. The chemical potential φ, measured relative to its transition value μ_0, and the displacement u are then both functions of x and t, $\varphi(x,t) := \mu(x,t) - \mu_0$ and $u(x,t)$. At time t, the interface is identified with a point located at $\xi(t)$, and the α phase occupies the subinterval $(0, \xi(t))$ while the β phase occupies the subinterval $(\xi(t), 1)$. We shall restrict our attention to bulk grand canonical potentials that are quadratic in strain and affine in diffusion potential:

$$\omega_i(\mu, \varepsilon) := \frac{1}{2} E_i (\varepsilon - \varepsilon_i^\circ)^2 - \Lambda_i \varphi \quad (i = \alpha, \beta), \tag{13}$$

where E_i is the Young modulus of the i phase and the constant strain ε_i° represents its *natural state*, i.e.,

$$\sigma_i(\mu, \varepsilon_i^\circ) := \frac{\partial \omega_i(\mu, \varepsilon_i^\circ)}{\partial \varepsilon} = 0, \tag{14}$$

and the transition potential μ_0 satisfies

$$\omega_\alpha(\mu_0, \varepsilon_\alpha^\circ) = \omega_\beta(\mu_0, \varepsilon_\beta^\circ) = 0. \tag{15}$$

The difference $\varepsilon_\beta^\circ - \varepsilon_\alpha^\circ$ represents the *misfit strain* between the natural states of the individual phases. (Note that the *linear* dependence of the grand canonical potential of each of the two phases on the chemical-potential difference is consistent with the assumption that the latter is *small*. The equations that derive from (13) are therefore appropriate for small departures of the solute potential from its transition value.)

We wish to investigate the growth of a seed of the α phase that initially occupies a single point. Specifically, we consider the initial condition

$$\xi(0) = 0, \tag{16}$$

so that the entire bar is initially in the β phase, the α phase being confined to the endpoint $x = 0$. As mechanical and chemical boundary conditions, we assume that the left endpoint of the bar is pinned and impermeable to the diffusing species,

$$u_\alpha(0, t) = \frac{\partial \varphi_\alpha(0, t)}{\partial x} = 0, \tag{17}$$

while the right endpoint is subjected to an axial dead load σ^* and in contact with a reservoir at constant relative chemical potential φ^*,

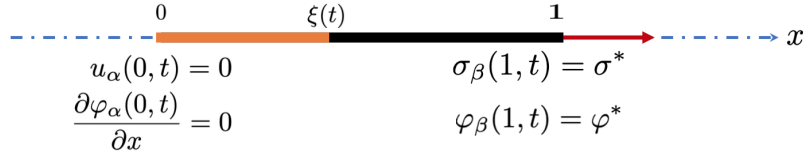$$\sigma_\beta(1, t) = \sigma^* \quad \text{and} \quad \varphi_\beta(1, t) = \varphi^*. \tag{18}$$

Figure 4: Schematic of a two-phase linearly elastic bar, with the phase α, shown in orange, growing at the expense of the β phase, shown in black. At time t, the phase boundary, whose evolution is governed by the interplay between solute diffusion and mechanical stress, is located at $\xi(t)$. The left endpoint $(x = 0)$ is pinned and impermeable to the diffusing solute, while a dead load σ^* is applied at the right endpoint $(x = 1)$, assumed in contact with a solute reservoir whose constant potential difference is φ^*.

2.1. Specializing the equations derived in class to the one-dimensional setting at hand, formulate the free-boundary problem whose unknowns are the displacements $u_\alpha(x, t)$ and $u_\beta(x, t)$, the potential differences $\varphi_\alpha(x, t)$ and $\varphi_\beta(x, t)$ of the diffusing species, and the position $\xi(t)$ of the phase boundary.

2.2. Show that the equations that govern the displacement field *decouple* from those that determine the evolution of the chemical potential of the diffusing species, and that the former can be solved *independently* from the latter. Compute the stress, strain, and displacement fields in each of the two phases.

2.3. Using the results of the previous question, determine the potential differences $\varphi_\alpha(x, t)$ and $\varphi_\beta(x, t)$, and write the differential equation that the interfacial position $\xi(t)$ has to satisfy.

2.4. Depending on the signs of the jump $\Lambda := \Lambda_\beta - \Lambda_\alpha$ in solute densities between the two phases, the misfit strain $\varepsilon^\circ := \varepsilon_\beta^\circ - \varepsilon_\alpha^\circ$, and the difference $E := E_\beta - E_\alpha$ in Young's moduli of the two phases, determine when the phase transformation (by which the β phase grows at the expense of the α phase) can occur, i.e., the conditions that φ^* and σ^* have to satisfy for the phase boundary to propagate into the α phase.

2.5. Finally, assuming that the conditions found in the previous question are satisfied, determine the position $\xi(t)$ of the phase boundary at time t and compute the time t^* needed for the entire bar to transform from the α phase into the β one.